Modeling of the adsorption on Cr_2O_3 clusters of small molecules and ions present in seawater. A preliminary non-empirical study

C. Compere,[a] D. Costa,[b] L.-H. Jolly,[c] E. Mauger[c] and C. Giessner–Prettre*[c]

[a] *Service Matériaux et Structures, IFREMER, Centre de Brest, B.P. 70, 29280 Plouzane, France*
[b] *Laboratoire de Réactivité de Surface (CNRS UMR 7609), Université Pierre & Marie Curie, Case Courrier 168, 4, place Jussieu, 75252 Paris cedex 05, France*
[c] *Laboratoire de Chimie Théorique (CNRS UMR 7616), Université Pierre & Marie Curie, Case Courrier 137, 4, place Jussieu, 75252 Paris cedex 05, France*

Received (in Montpellier, France) 3rd July 2000, Accepted 18th August 2000
First published as an Advance Article on the web 14th November 2000

Non-empirical calculations of a Cr_2O_3 unit, taken as an initial model of chromium oxide clusters, interacting with ions and (small models of) molecules present in natural seawater have been carried out. The results obtained for the isolated oxide unit show that the coupling between the unpaired 3d electrons of the two chromium atoms has a negligible influence on the charge distribution. The results concerning the adsorption show that: (*i*) water, methanol and formic acid are dissociated; (*ii*) the chlorine anion, which is not strongly adsorbed, can easily be removed from the cluster; (*iii*) the Mg^{2+} adsorption energy is considerably larger than that of Na^+ and Ca^{2+}; (*iv*) the interaction energy of these cations is enhanced by Cr_2O_3 hydroxylation; (*v*) dissociated methanol and formic acid are, of all the molecules considered in this study, those having the strongest interaction energy with Cr_2O_3. In a very limited number of cases the computations were repeated for a larger cluster (Cr_4O_6), for a Cr_2O_3 cluster embedded in a set of point charges, or for a hydroxylated Cr_2O_3 unit, to study the influence of the environment on the binding energy and geometrical arrangements of the complexes.

A surface immersed in an aquatic environment is rapidly covered with a biological slime or biofilm.[1] Numerous laboratory as well as real-life experiments on materials immersed in seawater highlight different stages in the formation of the biofilm. The first, occuring within minutes of immersion up to a few hours, corresponds to the adsorption of organic and/or inorganic (macro-)molecules already present in the environment or produced by micro-organisms.[2,3] These adsorbed macro-molecules form the "primary film" or "conditioning film".

This layer is essential because the induced modifications of the surface properties (surface tension, surface free energy, polarity, wettability) will permit the subsequent adhesion of micro-organisms such as bacteria, fungi and algae. The marine fouling of structures and equipment is a major problem for industrial and scientific activities in the sea. Costly countermeasures are needed to avoid the adhesion of such micro-organisms and local pollution results from extensive use of inappropriate antifouling techniques. Indeed, an improved knowledge of biofilm adhesion mechanisms is essential to develop an alternative approach to the currently used antifouling agents.

Thus, the BASIS (Biofilm Adhesion on Surfaces Immersed in Seawater) group, involving several laboratories in different fields of research (material science, chemistry, marine microbiology, biochemistry and theoretical chemistry) has focused its efforts on the characterization of the primary film formed on a 316L stainless steel surface in the first hours of immersion in natural seawater. The main results obtained from the experimental approach are the following:[4–6] (*i*) The alloy surface is covered by a 25 Å mixed (Fe^{3+}, Cr^{3+}) oxide layer, chromium oxide being markedly predominant after longer immersion times. The presence of hydroxyl groups and/or H_2O molecules is observed on the surface of this layer.[7–9] (*ii*) Adsorption of organic matter (proteins and carbohydrates) occurs on the surface of the alloy and is evidenced by experimental techniques (X-ray photoelectron spectroscopy, infrared reflection absorption spectroscopy, time-of-flight secondary ion mass spectroscopy, atomic force microscopy); the quantity of matter adsorbed on the surface increases with immersion time during the first 24 h. (*iii*) The procedure adopted for surface preparation, in particular the cleaning procedure with solvents, may influence the kinetics of formation of the primary film. (*iv*) This primary film is not a continuous one. Even after 24 h of immersion, the whole surface is not covered.[6] This result is of primary importance in relation to modeling studies since it suggests that organic matter adsorbs on specific sites of the surface (defects, inhomogeneities, *etc.*).

In order to get a deeper understanding of the first steps occuring during immersion in seawater, a theoretical approach has been undertaken. Because of the size and the complexity of the system of interest—an oxide surface of unknown exact structure interacting with water, ions and biomolecules—a semi-empirical method will have to be used in the future. In a preliminary study, the results of which are reported hereafter, we have performed *ab initio* calculations in order to get benchmarks to test the future semi-empirical results. We have chosen to model the stainless steel surface by chromium oxide Cr_2O_3 clusters, since at long immersion times the surface is known to be enriched in Cr_2O_3. Clusters appear to be a reasonable stainless steel surface model for several reasons: (*i*) the alloy surface has been polished and therefore does not have a defectless crystal-like surface; (*ii*) although the average thickness of the Cr_2O_3 film can be measured its homogeneity is not known; (*iii*) a cluster exhibits characteristics similar to those of defects and/or inhomogeneities of the surface at which adsorption of organic matter takes place. The available experimental data concerning adsorption on a pure Cr_2O_3 surface[7–9] as well as those concerning the interactions with stainless steel[10,11] will be used for comparison purpose. Therefore, we undertook the study of the interaction of water, cations and anions (potentially) present in seawater, such as Na^+, Mg^{2+}, Ca^{2+} and Cl^-,[12] and that of protein and carbohydrate functional groups with a Cr_2O_3 unit. Some of these computations were repeated for Cr_4O_6, for Cr_2O_3 surrounded by point charges, as well as for a hydroxylated Cr_2O_3 unit, in order to study the influence of the surroundings normally present in the real system. These results will not only be useful as benchmarks but also give indications on the possible role of these various entities in the formation of the primary film and therefore give hints on the structure of the ions/molecules/complexes to be considered as adsorbates in a future semi-empirical study.

Computational details

For all the calculations we have used the 6-31G basis set.[13,14] For the non-metal atoms the standard polarization and diffuse functions have been added.[15] They have been omitted on the chromium, sodium, calcium and magnesium atoms since they carry important positive charges and therefore, being more compact, do not require as large a basis as potentially anionic atoms in the entities under consideration. Except for some cases concerning Cr_2O_3, Cr_4O_6 and $Cr_2O_3H_2O$ the computations have been carried out at the ROHF level for the high spin state of the systems: that is a multiplicity of 7 or 13 for Cr_2O_3 and Cr_4O_6, respectively. In a very limited number of cases the computations have been repeated using B3LYP density functional[16] (ROB3LYP high spin) and ROHFMP2 to estimate the contribution of correlation to the calculated interaction energies and at the CASSCF level for the singlet. Because of computer limitations the CASSCF calculations were limited, with a single exception, to the six (twelve) unpaired chromium d electrons in the six (twelve) active orbitals for Cr_2O_3 and Cr_4O_6, respectively. Since Cr_2O_3 is antiferromagnetic the computations should in all cases be carried out using this computational level. However, for the time being, such calculations definitely cannot be run routinely for systems with several hundreds of atomic orbitals. These computations were undertaken to obtain an estimation of the possible error introduced by doing the calculations for the high spin state instead of the low spin one. In particular, we felt it necessary to assess the sensitivity of the charge distribution, a factor of primary importance in such "ionic" oxides, to the spin multiplicity considered. For Cr_2O_3 the CASSCF computations were repeated taking into account the 10 chromium d orbitals in the active space.

In three cases the calculation of the interaction energy of Cr_2O_3 with a molecule has been repeated for a cluster embedded in a set of point charges in order to probe the influence of the environment on the results. In these computations the point charges were located on the atomic sites of the nine Cr_2O_3 units surrounding the Cr_2O_3 unit being treated quantum mechanically. The charges used were +0.6 on the chromiums and −0.4 on the oxygens. These values were retained because they gave the best agreement for the electron population variations with those obtained from the full quantum mechanical treatment when going from Cr_2O_3 to Cr_4O_6 and Cr_6O_9. When using the Mulliken population for the second Cr_2O_3 unit of Cr_4O_6 the chromium charges and d orbital populations were equal to 1.608/3.637 and 1.948/3.771 for the two Cr atoms of the first Cr_2O_3, respectively, while they are 1.601/3.723 and 1.731/3.773 with the chosen set of point charges (see Table 1 for the comparison with the full quantum mechanical results).

The geometry of the Cr_2O_3 unit is taken from chromium oxide crystal data.[17] Since we are not dealing with a well-defined material it can be considered as a reasonable zeroth-order approximation of an oxide unit of the surface we are interested in. The geometry of the unit was kept fixed during the optimization of the geometrical arrangement of entities in interaction with the oxide. All the geometrical parameters (intra- and intermolecular) of the adsorbed entities were optimized. Since this study does not tend to determine adsorption energies but merely get a scale of interaction energies between clusters and various molecular and ionic species, the BSSE correction has been calculated in only one case. Its magnitude was found to be small enough not to modify the order of preferential adsorption.

The computations have been carried out using Gaussian 98[18] and HONDO 95.6.[19]

Results and discussion

The values concerning Cr_2O_3, reported in Table 1, show that the energies of the two spin states differ by less than 1 kcal mol^{-1}, since the energies of the septuplet and singlet are equal to −2310.8456 and −2310.8450 a.u., respectively. This small difference is in agreement with the small J value measured ($\approx$0.3 kcal mol^{-1}[20]). But the theoretical results from the CASSCF(6,6) calculation are in favor of the high spin electronic configuration while experiment shows that chromium oxide is antiferromagnetic. On the other hand the CASSCF-(6,10) computations, that is those introducing the 10 d orbitals of the chromium atoms, give energies of −2310.8516 and −2310.8540 a.u. for the high and low spin configurations, respectively, a result in complete agreement with experiment. We also see from Table 1 that if there are 3 unpaired d electrons on each chromium, since the spin density is greater than 2.9, the d orbital population is closer to d^4 than to d^3. It is worth noticing that the electron distributions are identical in the high (7) and low (1) spin states as can be seen from the

Table 1 Calculated characteristics of Cr_2O_3, Cr_4O_6 and Cr_6O_9 at different computational levels: energy (E), chromium charges (Q), chromium d orbital population ($3d^{pop}$); chromium spin densities (ρ) and occupation of the CASSCF singlet orbitals (Occ. Nb.)

Multiplicity			Cr_2O_3	Cr_4O_6	Cr_6O_9
7/13/19	ROHF	E/a.u.	−2310.8456	−4621.9218	−6933.0072
		Q	1.585	1.505–1.708	1.481–1.720
		$3d^{pop}$	3.780	3.666–3.807	3.662–3.810
		ρ	2.962	2.950–2.962	2.950–2.961
7/13	ROB3LYP	E/a.u.	−2314.4038	−4628.9996	[a]
		Q	1.060	1.120–1.266	[a]
		$3d^{pop}$	4.205	4.128–4.235	[a]
		ρ	2.962	2.860–2.908	[a]
1	CASSCF	E/a.u.	−2310.8450	−4621.9217	[a]
		Q	1.587	1.504–1.708	[a]
		$3d^{pop}$	3.779	3.665–3.809	[a]
		Occ. Nb.	0.9694–1.0402	0.9999–1.0012	[a]
		ρ	2.959	[a]	[a]

[a] Not calculated.

atomic net charges reported in Table 1. This equality, which is retained in the CASSCF(6,10) results, suggests that the interaction energy of Cr_2O_3 with adsorbed species should be very similar for both spin states. The results obtained from B3LYP computations show that when correlation is taken into account the polarity of the Cr–O bonds is significantly reduced through a charge transfer from the oxygens into the metal d orbitals since the chromium net charge decreases by 0.5 electrons and their d orbital population increases by the same amount. These variations are obtained from NBO as well as from Mulliken population analysis.

The values concerning Cr_4O_6, the geometry of the system being that of two nearest neighbor units in the crystal, show that the interaction tends, as expected, to increase the formal charge on the metal. We see also from the ROHF and ROB3LYP energy values for Cr_2O_3 and Cr_4O_6 that the calculated interaction energy between the two Cr_2O_3 units of the Cr_4O_6 cluster decreases from -149.2 to -120.5 kcal mol^{-1} when going from the HF to DFT computational level. This last result is in agreement with the decrease in polarity of the Cr–O bond due to electron correlation. The important decrease of the "binding" electrostatic contribution to the interaction energy, which proceeds from intramolecular correlation effects, is not compensated by the second-order dispersion forces. This variation is not an artifact due to the use of DFT instead of post Hartree–Fock treatments since ROHFMP2 runs give an interaction energy of -113.4 kcal mol^{-1}. For this system the values obtained for the high and low spin electronic confirgurations are very close, as in the case of Cr_2O_3. The energy difference is smaller than for Cr_2O_3. Therefore, it appears that both configuration interaction and interactions between Cr_2O_3 units do contribute to the stabilization of the low spin state. It is worth remarking that in the Cr_4O_6 dimer, as in the monomer, the electron distribution is very similar for the two spin states.

The values in Table 1 concerning Cr_6O_9 in the high spin state show that the increase of the cluster size further increases the chromium net charges and that the long range interaction between the two non-bonded Cr_2O_3 units stabilizes the cluster by -5.8 kcal mol^{-1}. For Cr_6O_9 the ROHMP2 calculation give an interaction energy of -232.5 instead of -295.2 kcal mol^{-1} at the ROHF level. This variation confirms the decrease of the electrostatic contribution to the interaction energy when correlation is taken into account.

The data concerning H_2O interacting with Cr_2O_3 are reported in Table 2 and depicted in Fig. 1. The tabulated values show that "dissociated" water is more stable than adsorbed water by -55 kcal mol^{-1} at the HF level, for the high as well as the low spin states, and by -32 kcal mol^{-1} when introducing correlation. The difference between these two values illustrates again the importance of the decrease of the ionic character of the Cr–O bonds due to correlation. However, this contribution is not large enough to invert the

Table 2 Calculated interaction energies (kcal mol^{-1}) of Cr_2O_3 with H_2O

		$Cr_2O_3OH^-H^+$		$Cr_2O_3H_2O$	
Method	Mult.	Isolated	Embedded	Isolated	Embedded
ROHF	7	-92.7	-110.6	-36.2	-46.6
CASSCF	1	-93.1		-36.2	
ROB3LYP	7	-60.1		-28.4	

stabilities of the two modes of interaction. These results are in complete agreement with experiment since several surface sensitive spectrocopies[7,8,21,22] have shown the presence of OH groups on chromium oxide surfaces after either exposure to water vapor or immersion in water. It has to be noted that the numerical values of the water adsorption energy obtained from our computations are somewhat smaller than those obtained by Bredow[23] using SINDO1,[24] which are in the range -41 to -56 kcal mol^{-1} for an embedded Cr_2O_3 (0001) surface. This suggests that the interaction energy values reported in Table 2 could be underestimated due to neglect of the environment/embedding in agreement with the value of 46.6 kcal mol^{-1} obtained with the embedding used in this study. In the case of dissociated water the values in Table 2 show that embedding increases the adsorption energy in that case also, but both sets of results indicate that dissociative adsorption is the most probable. The optimized arrangements depicted in Fig. 1 show that embedding modifies more significantly the orientation of the adsorbed water molecule when it is not dissociated. The results obtained for the adsorption of water on Cr_4O_6, depicted in Fig. 2, show that the interaction energy is smaller than the corresponding values for Cr_2O_3 when the adsorption takes place on a chromium bonded to four oxygens (-35.1 *vs.* -36.2 kcal mol^{-1} for Cr_2O_3 and -63.5 *vs.* -92.7 kcal mol^{-1} for Cr_2O_3) for the non-dissociative and the dissociative binding modes, respectively Fig. 2(a) and (b). On the contrary, we get a larger value of -101.7 kcal mol^{-1} (*vs.* -92.7 kcal mol^{-1} for Cr_2O_3) for dissociative adsorption when it occurs on a "surface chromium" that is bound to only three oxygens [Fig. 2(c)]. These results indicate that the adsorption is less favorable energetically when the chromium is bonded to more than three oxygens. The calculated values, at the HF level, of the interaction energy of $Cr_2O_3OH^-H^+$ with a water molecule of the second hydration shell is considerably weaker than that of Cr_2O_3 with a water, dissociated or not, of the first shell since we obtain -2.8 and -5.5 kcal mol^{-1} for the OH^-OH_2 and H^+OH_2 cases, respectively (see Fig. 3). In this case the calculated interaction energies are of the same order of magnitude as that between two water molecules (5.0 kcal mol^{-1} with the basis used in this study). The $CrOH^-OH_2$ interaction energy values are similar to those obtained by Kittaka *et al.*[22] for the interaction of water with three hydroxyl groups of $Cr(OH)_6$. On the other hand, the -2.8 kcal mol^{-1} value is in qualitative agreement with their experimental results, which suggest the existence of surface OHs that are inert towards H_2O adsorption.

The interaction energy and the optimized geometrical arrangements of Cr_2O_3 bound to the six anions considered in

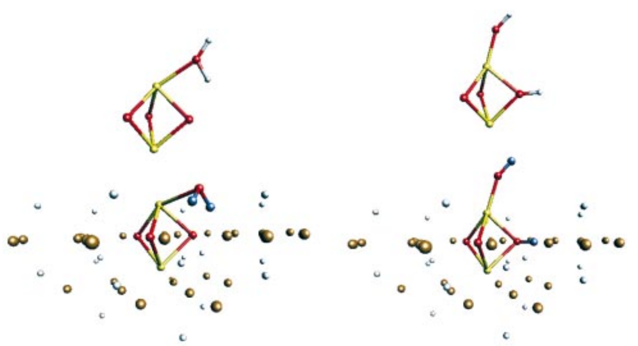

Fig. 1 Optimized structures of $Cr_2O_3H_2O$ showing associated (left) and dissociated (right) water in the isolated (upper) and embedded (lower) models. The darker circles correspond to the oxygen like point charges and the lighter to the chromium like ones.

a -35.1   b -63.5   c -101.7

Fig. 2 Optimized structures and interaction energies (kcal mol^{-1}) of $Cr_4O_6H_2O$.

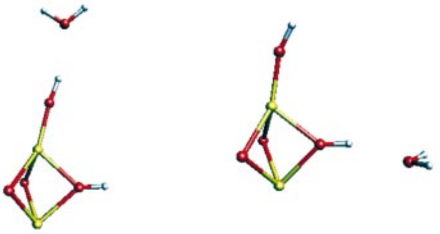

Fig. 3 Optimized structures of $Cr_2O_3(H_2O)_2$.

this study are displayed in Fig. 4. CH_3S^-, $HCOO^-$ and CH_3O^- are taken as models for the cysteine, aspartic/glutamic, and serine/threonine residue side chains. OH^- is added for comparison purposes. The reported values show that Cl^-, the anion with the highest concentration in seawater, has a weak interaction energy compared to the other anions considered with the exception of CH_3S^-. This result suggests that Cl^- is not able to subsitute an OH^- anion and will be easily removed from the surface by other anions. However, it should be noted that its interaction energy is larger than that of dissociated water. The value obtained for CH_3S^- does not support the hypothesis concerning the role of the thiol group in the deposition of β-lactoglobulin on chromium oxide[25] since $HCOO^-$ and CH_3O^-, which are also present in the protein, have larger interaction energies.

The calculated interaction energies of Cr_2O_3 with cations present in seawater (Na^+, Ca^{2+}, Mg^{2+}) or with $CH_3NH_3^+$, a model of the lysine side chain, are reported in Table 3 and Fig. 5 (H^+ is added for comparison purposes). The results concerning the atomic cations show that magnesium dication is the only one for which arrangement b (depicted in Fig. 5), which implies the interaction with two oxygen atoms, is more stable than arrangement a in which the cation interacts with only one oxygen. At this point it is interesting to note that Mg^{2+}, which has, in seawater, the highest concentration after sodium,[12] has the largest adsorption energy on the Cr_2O_3 surface after the proton. The interaction energy of Mg^{2+} with H_2O is -80.3 kcal mol^{-1}. Thus, the loss of one water molecule in the Mg^{2+} hydration shell to permit the binding of the cation on the oxygen of Cr_2O_3 is energetically favorable. The values reported in Table 3 tend to show that sodium cations adsorbed on Cr_2O_3 are easily replaced by other cationic species. However, we have to stress that a proton, especially when interacting with only one oxygen, is definitely the most strongly bound species, therefore it is unlikely to be replaced by another cation. On the other hand, the relatively small value calculated for the interaction with $CH_3NH_3^+$ is in agreement with the low coverage measured for poly-L-lysine on stainless steel.[10]

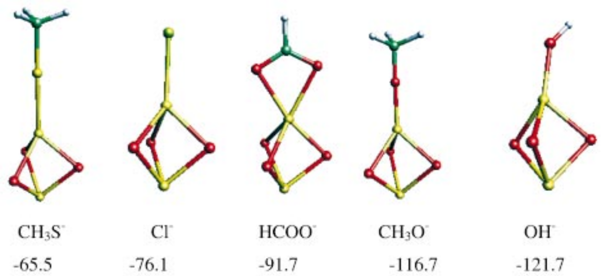

Fig. 4 Optimized structures and interaction energies (kcal mol^{-1}) of Cr_2O interacting with anions.

Table 3 Calculated interaction energy (kcal mol^{-1}) of Cr_2O_3 with cations

	Geometrical arrangement (see Fig. 5)	
Cation	a or c	b or d
Na^+	-47.9	-47.9
Ca^{2+}	-110.9	-106.1
Mg^{2+}	-168.5	-170.6
H^+	-266.8	-198.2
$CH_3NH_3^+$	-32.2	-54.3

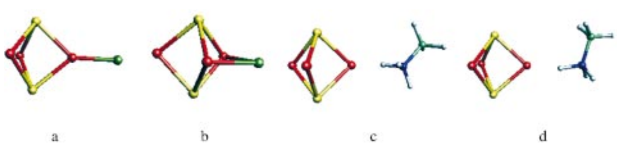

Fig. 5 Geometrical arrangement of Cr_2O_3 interacting with cations: (a) cation bound to one oxygen; (b) cation bound to two oxygens; (c) $CH_3NH_3^+$ bound by one NH proton; (d) $CH_3NH_3^+$ bound by two NH protons.

These results led us to consider the interaction of Na^+, Ca^{2+} and Mg^{2+} with a hydroxylated Cr_2O_3 unit. In this case the interaction energies are enhanced by 30–40% with respect to their value for bare Cr_2O_3. We see from Fig. 6 that in the optimized geometrical arrangements the cations are interacting with the oxygen of the OH^- and an oxygen of the Cr_2O_3 unit. This is possible because of the flexibility of the Cr–OH bond. It is worth noting that the global interaction energy in the system $Cr_2O_3H_2OMg^{2+}$ is -313.8 kcal mol^{-1}.

The results concerning the interaction of Cr_2O_3 with neutral molecules are reported in Fig. 7. The values reported show that ethane, taken as a model for hexane, used for rinsing the surface, on the one hand, and of the side chain of the aliphatic amino acids (valine, isoleucine, *etc.*) on the other, has the smallest interaction energy. Methyl ether, taken as a first model for the carbohydrate ether group, is the next most strongly bound molecule. For *cis*-*N*-methyl formamide, taken as a model for the protein backbone and the aspargine and glutamine side chains, our results indicate that the adsorption can take place either through the carbonyl oxygen lone pairs or through the carbonyl π electrons, as can be seen from Fig. 7(c) and (d). This result indicates that the adsorption of peptide groups on the chromium atoms of a Cr_2O_3 surface will undergo little steric hindrance. Imidazole, a model for the histidine side chain, has an interaction energy value close to that of the peptide group. The results concerning methanol and formic acid, taken as models for the threonin/tyrosin and glutamic/aspartic side chains, show that these molecules will dissociate on Cr_2O_3 and are able to replace dissociated water, which has an interaction energy some 20 kcal mol^{-1} smaller. This result shows that molecules with alcohol and/or carboxyl functional groups will be those with the largest adsorption energy on a Cr_2O_3 cluster. It is worth mentioning that with the embedding used for water the interaction energy of dissociated formic acid is -135.9 kcal mol^{-1} that is 25 kcal mol^{-1} larger than dissociated water, while the interaction energies of dissociated water and methanol with a hydroxylated Cr_2O_3 unit are -39.8 and -58.7 kcal mol^{-1}, respectively. This set of values indicates that if the calculated interaction energy values between the adsorbates and an isolated Cr_2O_3 unit are most probably not numerically satisfactory since they are overestimated, the relative ordering of their affinity toward the oxide is correctly given by these calculations. The results concerning

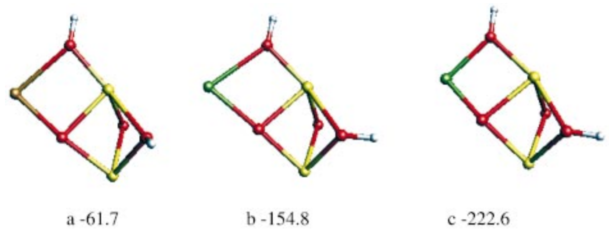

Fig. 6 Optimized arrangements and interaction energies (kcal mol^{-1}) of $Cr_2O_3OH^-H^+$ with: (a) Na^+, (b) Ca^{2+}, (c) Mg^{2+}.

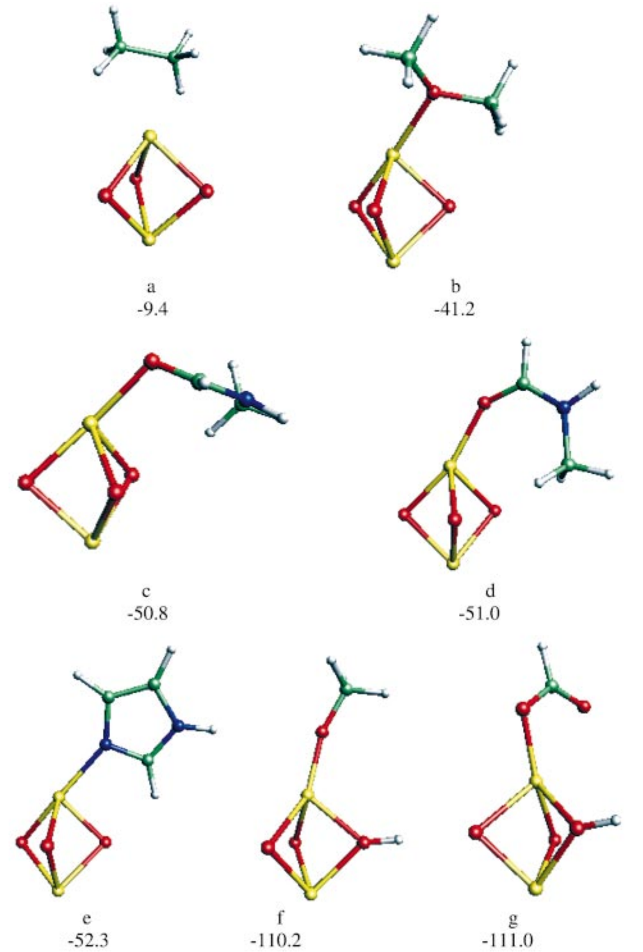

Fig. 7 Optimized arrangements and interaction energies (kcal mol^{-1}) of Cr_2O_3 interacting with: (a) ethane, (b) methyl ether, (c) and (d) *N*-methylformamide, (e) imidazole, (f) methanol, (g) formic acid.

methanol and formic acid seem to be in qualitative agreement with experimental data since the formation of alkoxides[26] has been observed on hydroxylated chromium oxide as well as that of complexes between oxalic acid and chromium hydrous oxide.[27] Absorption of 3,4-dihydroxybenzoic acid on stainless steel surfaces has also been observed.[10]

Conclusion

The present work is the first step in the modeling of the interactions of a chromium oxide surface with several entities present in seawater. Despite the unavoidable oversimplification of the studied system, the results obtained are in reasonable agreement with the available experimental data. Thus, our calculations do find six unpaired d electrons in Cr_2O_3 with a small coupling between the two chromiums, the dissociation of water and the formation of alkoxides on this oxide. We think that these results can give useful indications on the functional groups/ions responsible for the adsorption of bio(in)organic material on stainless steel in seawater. The present results show clearly that sodium chloride should not contribute significantly to the formation of the biofilm since it will be easily removed from the surface. On the other hand, the large interaction energy found for Mg^{2+} suggests that this cation might modify the charge of the surface at some sites. Maybe more important in relation to the formation of the biofilm is the large interaction energy obtained for dissociated alcohol and carboxyl groups, which appear to be able to replace the dissociated water molecules adsorbed on the surface. Since both functional groups are present in proteins and the former in carbohydrates, our results suggest that they might be responsible for the rapid adsorption of these biomolecules as experimentally observed. The importance of the role of carboxylic and alcoholic functional groups in the adsorption of proteins on stainless steel has also been stressed on experimental grounds.[10,11] The results concerning a hydroxylated Cr_2O_3 unit show that if the numerical values of the interaction energies are significantly modified by the presence of the dissociated water molecule, the relative order of the adsorption energies of the different species considered is not modified by the state of hydration of the surface. Therefore, we believe that the present study shows clearly that alcohol and carboxyl groups, on the one hand, and magnesium cations, on the other, are of primary importance in the formation of the conditioning film on stainless steel in natural seawater.

Acknowledgements

We thank the Centre de Calcul Recherche of the Université P. & M. Curie and IDRIS (CNRS) for computer time.

References

1 G. E. Brown, Jr., V. E. Henrich, W. H. Casey, D. L. Clark, C. Eggleston, A. Felmy, T. W. Goodman, M. Grätzel, G. Maciel, M. I. McCarthy, K. H. Nealson, D. A. Sverjensky, M. F. Toney and J. M. Zachara, *Chem. Rev.*, 1999, **99**, 77.
2 R. Neihof and G. Loeb, in *Proceedings of the Third International Congress on Marine Corrosion and Fouling*, National Bureau of Standards, Gaithersburg, MD, 1972, p. 710.
3 R. E. Baier, in *Proceedings of the Third International Congress on Marine Corrosion and Fouling*, National Bureau of Standards, Gaithersburg, MD, 1972, p. 633.
4 D. Costa, P. Marcus, M.-N. Bellon–Fontaine, B. Rondot, M. Walls, O. Vidal, P. Lejeune and C. Compere, in *Proceedings of the Symposium on Passivity and its Breakdown, Joint ECS/ISE Meeting*, ed. P. Natishan, H. S. Isaacs, M. Janik–Czachor, V. A. Macagno, P. Marcus and M. Seo, The Electrochemical Society Proceedings Series, PV 97-26, The Electrochemical Society, Pennington, NJ, 1998, pp. 450–461.
5 M. G. Walls, B. Rondot, D. Costa, C.-M. Pradier, P. Marcus, M.-N. Bellon–Fontaine, C. Compere and J. Guezennec, in *Proceedings Euromat 98* (*Materials in Oceanic Environment*), ed. L. Faria, Sociedade Portugesa de Materiais, Lisbon, Portugal, 1998, vol. 1, pp. 421-430.
6 C.-M. Pradier, P. Bertrand, M.-N. Bellon–Fontaine, C. Compere, D. Costa, P. Marcus, C. Poleunis, B. Rondot and M. G. Walls, *Surf. Interface Anal.*, 2000, **30**, 45.
7 C. A. Ventrice, Jr., D. Ehrlich, E. L. Garfunkel, B. Dillmann, D. Heskett and H.-J. Freund, *Phys. Rev. B*, 1992, **46**, 12882.
8 D. Cappus, C. Xu, D. Ehrlich, B. Dillman, C. A. Ventrice, Jr., K. Al Shamery, H. Kuhlenbeck and H.-J. Freund, *Chem. Phys.*, 1993, **177**, 533.
9 D. Costa, M. P. Yang and P. Marcus, *Mater. Sci. Forum*, 1995, **185–188**, 325.
10 D. C. Hansen, G. W. Luether, III and J. H. Waite, *J. Colloid Interface Sci.*, 1994, **168**, 206.
11 S. Omanovic and S. G. Roscoe, *Langmuir*, 1999, **15**, 8315.
12 Artificial seawater, Norm ASTM D1141-90, American Society for Testing and Materials, Philadelphia, PA.
13 W. J. Hehre, R. Ditchefield and J. A. Pople, *J. Chem. Phys.*, 1972, **56**, 2257.
14 V. A. Rassolov, J. A. Pople, M. A. Ratner and T. L. Windus, *J. Chem. Phys.*, 1998, **109**, 7764.
15 T. Clark, J. Chandrasekhar, G. W. Spitznagel and P. v. R. Schleyer, *J. Comput. Chem.*, 1983, **4**, 294.
16 (*a*) C. Lee, W. Yang and R. G. Parr, *Phys. Rev. B*, 1988, **37**, 785; (*b*) B. Miehlich, A. Savin and H. Preuss, *Chem. Phys. Lett.*, 1989, **157**, 200; (*c*) A. D. Becke, *J. Chem. Phys.*, 1993, **98**, 5648.
17 P. D. Battle, T. C. Gibb, S. Nixon and W. T. A. Harrison, *J. Solid. State Chem.*, 1988, **75**, 21.
18 M. J. Frish, G. W. Trucks, H. B. Schelgel, G. E. Scuseria, M. A. Robb, J. R. Cheeseman, V. G. Zakrzewski, J. A. Montgomery, Jr., R. E. Stratman, J. C. Burant, S. Dapprich, J. M. Millam, A. D. Daniels, K. N. Kudin, M. C. Strain, O. Farkas, J. Tomasi, V. Barone, M. Cossi, R. Cammi, B. Mennucci, C. Pomelli, C. Adamo, S. Clifford, J. Ochterski, G. A. Petersson, P. Y. Ayala, Q. Cui, K. Morokuma, D. K. Malick, A. D. Rabuck, K. Raghava-

chari, J. B. Foresman, J. Ciolowski, J. V. Ortiz, A. G. Baboul, B. B. Stefanov, G. Liu, A. Liashenki, P. Piskorz, I. Komaromi, R. Gomperts, R. L. Martin, D. J. Fos, T. Keith, M. A. Al-Laham, C. Y. Peng, A. Nanayakkara, C. Gonzalez, M. Challacombe, P. M. W. Gill, B. Johnson, W. Chen, M. W. Wong, J. L. Andres, C. Gonzales, M. Head–Gordon, E. S. Reploge and J. A. Pople, GAUSSIAN 98, rev. A.7, Gaussian, Inc., Pittsburgh, PA, 1998.
19 M. Dupuis, A. Marquez and E. R. Davidson, HONDO 95.6, IBM Corporation, Kingston, NY, 1995.
20 E. J. Samuelsen, M. T. Hutchings and G. Shirane, *Physica*, 1970, **48**, 13.
21 V. Maurice, S. Cadot and P. Marcus, *Surf. Sci.*, 2000, **458**, 195.
22 S. Kittaka, T. Sasaki, N. Fukuhara and H. Kato, *Surf. Sci.*, 1993, **282**, 255.
23 T. Bredow, *Surf. Sci.*, 1998, **401**, 82.
24 T. Bredow, G. Geudtner and K. Jug, *J. Chem. Phys.*, 1996, **105**, 6395.
25 T. Jeurnink, M. Verheul, M. Cohen Stuart and C. G. de Kruif, *Colloids Surf. B*, 1996, **6**, 291.
26 S. Kittaka, T. Umezu, H. Ogawa, H. Maegawa and T. Takenaka, *Langmuir*, 1998, **14**, 832.
27 J. Degenhardt and A. J. McQuillan, *Chem. Phys. Lett.*, 1999, **311**, 179.